

# SCIENTIFIC REPORTS



OPEN

## Centrin-2 (Cetn2) mediated regulation of FGF/FGFR gene expression in *Xenopus*

Jianli Shi, Ying Zhao, Tyson Vonderfecht, Mark Winey & Michael W. Klymkowsky

Received: 28 October 2014

Accepted: 27 March 2015

Published: 27 May 2015

Centrins (Cetns) are highly conserved, widely expressed, and multifunctional  $\text{Ca}^{2+}$ -binding eukaryotic signature proteins best known for their roles in ciliogenesis and as critical components of the global genome nucleotide excision repair system. Two distinct Cetn subtypes, Cetn2-like and Cetn3-like, have been recognized and implicated in a range of cellular processes. In the course of morpholino-based loss of function studies in *Xenopus laevis*, we have identified a previously unreported Cetn2-specific function, namely in fibroblast growth factor (FGF) mediated signaling, specifically through the regulation of FGF and FGF receptor RNA levels. Cetn2 was found associated with the RNA polymerase II binding sites of the Cetn2-regulated FGF8 and FGFR1a genes, but not at the promoter of a gene (BMP4) whose expression was altered indirectly in Cetn2 morphant embryos. These observations point to a previously unexpected role of Cetn2 in the regulation of gene expression and embryonic development.

Centrins (Cetn) are calmodulin-like eukaryotic signature proteins<sup>1</sup>. Cetn2-like and Cetn3-like subclasses of Cetns have been identified<sup>2,3</sup>. In the yeast *Saccharomyces cerevisiae* there is a single Cetn3-like *Cetn* gene, *CDC31*; its function is required for spindle pole body duplication<sup>4</sup>. The ciliated protozoa *Tetrahymena thermophila* contains (at least) four *Cetn* genes, three of which are expressed<sup>5</sup>.

Loss of either the Cetn2-like *Cen1* or the Cetn3-like *Cen2* genes produce non-redundant defects in basal body and cilia formation. While the Cetn2-like gene is essential for cell division, the Cetn3-like gene is not; cells null for the Cetn3-like *Cen2* gene appear to divide normally but have aberrant basal body organization<sup>5-7</sup>.

The roles of Cetns in vertebrate cells appear to be more subtle and diverse. Mice have four distinct *Cetn* genes; *Cetn2*, *Cetn3*, and *Cetn4* are typical intron containing genes, while *Cetn1* lacks introns and is thought to have been generated by a retrotransposition event from *Cetn2*<sup>8</sup>. Humans appear to lack a *Cetn4*-like gene<sup>9</sup>. Null mutations in mouse *Cetn1* lead to infertility apparently due to defects in sperm development<sup>10</sup>. Zebrafish *Cetn2* morphants<sup>11</sup> and mice homozygous for a null mutation in *Cetn2*<sup>12</sup> have no reported cell division phenotypes but display ciliopathy-related phenotypes. *Cetn3* and *Cetn4* null phenotypes in the mouse have not, to our knowledge, been reported.

The removal of all three *Cetn* genes has been achieved in the chick hyper-recombinogenic DT40 cell line. *Cetn2*, *Cetn3*, and *Cetn4* DT40 null cells display **no** apparent defects in centrosome formation or cell division but were hypersensitive to UV irradiation<sup>13</sup>. The radiation-sensitive phenotype observed in these cells was expected given the role of Cetn2 as an integral component of the nucleotide excision repair/xeroderma pigmentosum group C (XPC-RAD23-CETN2) complex<sup>14,15</sup>. Araki *et al.* reported that “almost 100% of CEN2 (sic) in the cell extract was co-precipitated with the anti-XPC antibody”<sup>14</sup>. While Cetns are certainly associated with centrosomes and basal bodies, the majority of cellular Cetn2 is apparently soluble and located throughout the cytoplasm and nucleus<sup>16</sup>. A number of other functions have been ascribed to Cetns, from the transport of heterotrimeric transducin G-proteins in retinal photoreceptor cells to interactions with heat shock proteins, the regulation of proteasome activity, and the nuclear

Molecular, Cellular & Developmental Biology University of Colorado Boulder, Boulder, Colorado 80309  
Correspondence and requests for materials should be addressed to M.W.K. (email: michael.klymkowsky@colorado.edu)

transport of RNAs and proteins<sup>3</sup>. It is clear that *Cetn2* and *Cetn3* have distinct functional roles in a number of systems.

## Results and Discussion

The idiosyncratic aspects of *X. laevis* development can reveal gene functions hidden in other organisms<sup>17</sup>. We therefore set out to explore the roles of *Cetns* in early *X. laevis* development. Both *X. laevis* and *X. tropicalis* have multiple centrin genes, based on data accessed through Xenbase<sup>18</sup>. The gene/protein originally designated as Centrin (*X. laevis*: NCBI Reference Sequence: NP\_001081398.1 and *X. tropicalis*: NP\_001016387.1) or Centrin-1 (*X. laevis*: NCBI Reference Sequence: NP\_001080127.1) display a *Cetn2*-like, rather than a *Cetn1*-like, genomic structure (see **supplementary figure 1**); we therefore refer to them as *Cetn2* (see below). No *Cetn1*-like gene appears to be present in either *X. laevis* or *X. tropicalis* genomes. The *Cetn3* and *Cetn4* genes identified in *X. laevis* are similar in genomic structure to those found in mouse and human.

The latest version of the *X. laevis* genome (7.1 as searched through the Xenbase Blast function in March 2015) reveals two distinct *Cetn2* (*Cetn2a* and *Cetn2s*) and *Cetn3* (*Cetn3l* and *Cetn3s*) genes, and apparently a single *Cetn4* gene. Our studies focus on the *Cetn2a*, *Cetn3l*, and *Cetn4* genes. *Cetn2a* corresponds to the 172 amino acid polypeptide labeled *centn1* or centrin (see above); *Cetn3l* corresponds to the 167 amino acid polypeptide labeled *Cetn3* (GenBank: AAI29791.1). We isolated full length cDNAs that correspond to *Cetn2a*, *Cetn3l*, and *Cetn4*. An analysis of gene expression during early *Xenopus* embryogenesis by Yanai *et al.*<sup>19</sup> (Fig. 1A) and our own RT-PCR data in *X. laevis* (Fig. 1B) indicate that *Cetn2a*, *Cetn3l*, and *Cetn4* RNAs are supplied maternally and are present at high levels throughout early development; we have not directly examined the expression levels of the *Cetn2s* or *Cetn3s* genes.

We used two different antibodies to localized *Cetn* proteins in *X. laevis*. The first is a rabbit antibody (anti-XlCetn)<sup>20</sup> that recognizes *Cetn2*, *Cetn3*, and *Cetn4* proteins based on its recognition of *Cetn2a*, *Cetn3l*, and *Cetn4* polypeptides expressed from injected RNAs (Fig. 1C and data not shown). The second antibody is a commercially available rabbit antibody (anti-HsCetn1) that reacts preferentially with *X. laevis* *Cetn2a* compared to *Cetn3l* (Fig. 1C). Because the anti-HsCetn1 antibody produced higher overall background labelling, we used the anti-XlCetn antibody for most staining studies. Both anti-*Cetn* antibodies stain the basal body region of epidermal ciliated cells (Fig. 1D–F). There is also discernible staining of the myotome; neuronal microtubules are not stained (Fig. 1G–J - anti-XlCetn staining shown). Basal body localization of all three *Cetns* was confirmed using C-terminally GFP tagged forms of *Cetn2a*, *Cetn3l*, and *Cetn4* expressed from injected RNAs (see below).

To down-regulate the levels of specific *Cetn* proteins in embryos we commissioned Gene-Tools LLC to design anti-sense translation blocking modified DNA oligonucleotides (morpholinos or MOs) specific for *Cetn2a*, *Cetn3l*, and *Cetn4* RNAs (see **supplemental figure. 2**). The *Cetn2s* gene encodes a 201 amino acid long polypeptide that differs from *Cetn2a* primarily by the presence of a 29 amino acid insertion at its N-terminus. Similarly the *Cetn3s* gene encodes a 212 amino acid long polypeptide that differs from *Cetn3l* primarily by the presence of a 32 amino acid insertion at its N-terminus. Given the dramatic nature of the *Cetn2* morphant phenotype (see below) we commissioned a second, completely non-overlapping anti-*Cetn2* morpholino (*Cetn2*-MO2). The translation of the *Cetn2s* RNA is not expected to be altered by either of the *Cetn2a* morpholinos used in our studies; similarly expression of *Cetn3s* is not expected to be altered by the *Cetn3l* morpholino. Because of its dramatic nature, we concentrate the studies described here on the characterization of the *Cetn2a* morphant phenotype. Plasmids that encode versions of *Cetn2a*-GFP, *Cetn3l*-GFP, and *Cetn4*-GFP that contain sequences that match the *Cetn2a*-MO1, *Cetn3l*-MO, and *Cetn4*-MO morpholinos perfectly were created for specificity and rescue studies. The *Cetn2*-MO1 and *Cetn2*-MO2 morpholinos reduced the level of *Cetn2* protein but not *Cetn3* or *Cetn4*, while the *Cetn3* and *Cetn4* morpholinos specifically reduced the accumulation of their targets (Fig. 2).

In ectodermal explants, a single *Cetn* morpholino alone (10 ngs/embryo) did not dramatically or reproducibly disrupt the formation of cilia in multiciliated cells; cilia formation did appear to be disrupted when multiple *Cetn* morpholinos were used together (**supplemental figure. 3** and data not shown). *Cetn2* morphants exhibited embryonic phenotypes unlike those associated with a typical ciliopathy; they appeared similar to those associated with defects in FGF-mediated mesoderm formation<sup>21</sup>. This phenotype was distinct from that displayed by *Cetn3* and *Cetn4* morphants (**supplemental figure. 3** and data not shown) as well as in Chibby (Cby) morphants (Cby is a basal body protein associated with the regulation of Wnt signaling)<sup>22</sup>.

To test whether *Cetn2* morpholinos disrupted FGF signaling, we used ectodermal and mesodermal explants, as described previously<sup>23</sup>. In culture, such explants normally elongate and form notochordal tissue within the mesodermal domain (Fig. 3A). When the mesodermal domain was taken from a *Cetn2* morphant embryo, elongation was inhibited and notochordal tissue failed to form (Fig. 2B). When the ectodermal region was derived from a *Cetn2* morphant, morphological extension was somewhat suppressed but notochordal tissue formed (Fig. 3C). Similar results were obtained using mesoderm only explants. Again, control explants displayed an extended morphology (Fig. 3D) and formed notochordal tissue (Fig. 3I). *Cetn2* morphant explants failed to elongate (Fig. 3E) or form notochord (Fig. 3J). The morphological extension and notochord phenotypes displayed by *Cetn2* morphant explants were rescued by *Cetn2* (Fig. 3G,K) but not by *Cetn3* (Fig. 3L) RNA injection. The *Cetn2* morpholino elongation defect

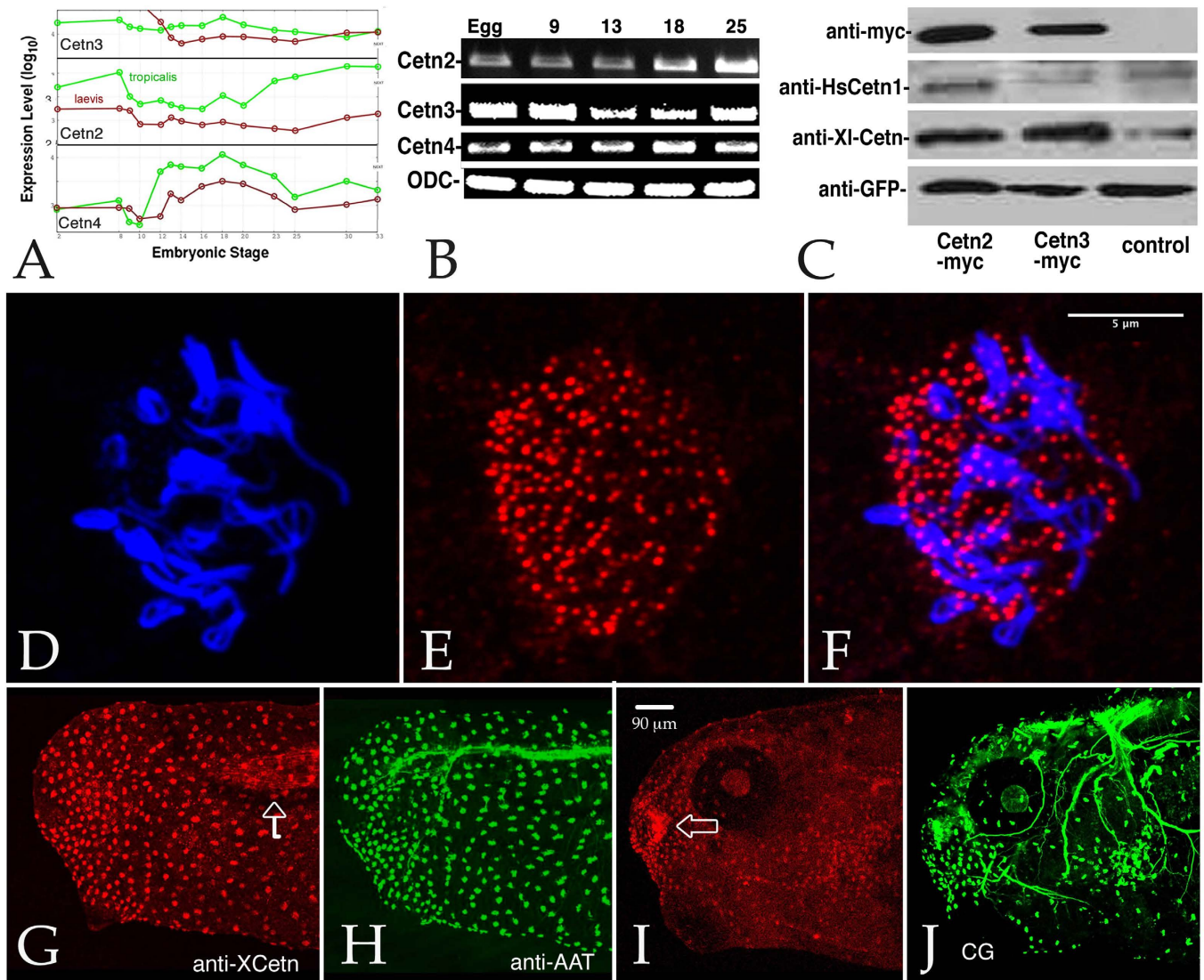


**Figure 1.** **A:** All three *Cetn* RNAs are present throughout the course of early development (data derived from Yanai *et al.* (2011)). **B:** This result was confirmed by RT-PCR analyses of *Cetn2a*, *Cetn3l*, and *Cetn4* RNAs using ornithine decarboxylase (*ODC*) as a normalization control (embryonic stages are noted). **C:** Embryos injected with RNA (200 pg) encoding GFP alone or together with *Cetn2a-myc* or *Cetn3l-myc* were harvested at stage 11 and analyzed by SDS-PAGE-immunoblot. The anti-human *Cetn1* antibody reacted preferentially with *X. laevis* *Cetn2*, while the anti-Xl*Cetn* antibody reacted with *Cetn2* and *Cetn3*, as well as *Cetn4* (data not shown). Ectodermal explants were fixed when sibling control embryos reached stage 18 and stained with anti-acetylated  $\alpha$ -tubulin (*AAT*)(**D**) and anti-Xl*Cetn* antibodies (**E**; **F** displays the overlap of images in parts **D** and **E**); this revealed the localization of *Cetns* to the basal body region of cilia. A similar analysis was carried out on whole embryos (**G,H** - stage 25, **I,J**-stage 35) stained with anti-Xl*Cetn* (**G,I**) and anti-acetylated  $\alpha$ -tubulin (**H,J**). Anti-*Cetn* staining of the myotome (arrow in part **G**) and *Cetn*'s localization to the olfactory region of the later stage embryo (arrow in part **I**) was obvious, as was its absence from the cement gland ("CG" in part **J**). Scale bar in part **F** marks 5  $\mu$ m in parts **D-F**, scale bar in part **I** marks 90  $\mu$ m in parts **G-J**.

was similar to that seen in explants derived from embryos injected with RNA encoding a dominant negative form of FGF Receptor 1 (*dnFGFR1*)(Fig. 3F). That the *Cetn2* morphant phenotype involves effects on FGF signaling was further suggested by the fact that the phenotype could be rescued by the injection of *FGF8* RNA (Fig. 3M).

Together with retinoic acid, Wnt, FGF, and BMP are three of the most prominent signaling pathways involved in early embryonic patterning, including mesoderm/notochord formation<sup>24</sup>. A preliminary RT-PCR analysis of the levels of *Wnt8a*, *FGF8* and *BMP4a* RNAs in stage 11 control and *Cetn2* morphant embryos revealed a dramatic decrease in *FGF8* and an increase in *BMP4a* RNA levels, with no apparent



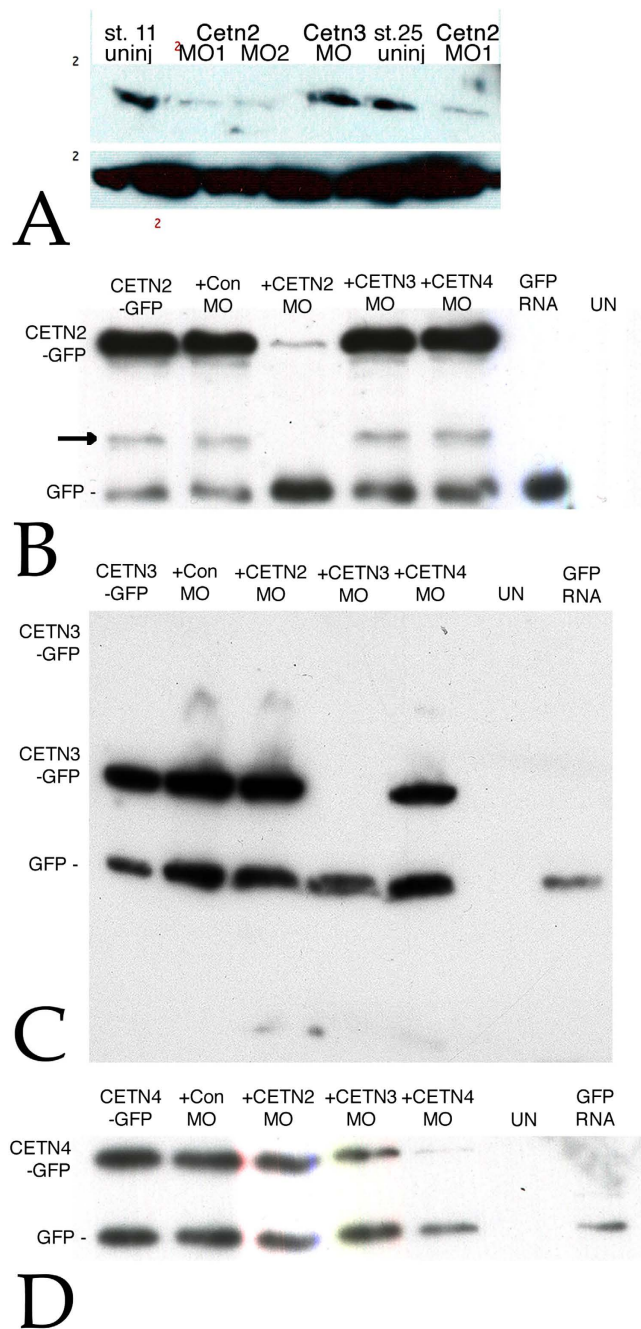


**Figure 2.** **A:** Embryos were injected into both cells at the two cell stage with RNAs encoding GFP (150 pgs per embryo) either alone or together with *Cetn2*MO1, *Cetn2*MO2, or *Cetn3*MO (10 ngs/side, 20 ngs total per embryo); at stage 11 or 25 the embryos were analyzed by SDS-PAGE and immunoblot using the anti-Human *Cetn-1* antibody (which reacts preferentially with *Cetn2* compared to *Cetn3*). There was a clear decrease in *Cetn2* protein levels, persisting through stage 25. To confirm the specificities of the *Cetn* MOs both blastomeres of two cell embryos were injected with RNAs encoding GFP (200 pg/side) and RNAs encoding *Cetn2a*-GFP (**B**), *Cetn3*-GFP (**C**), or *Cetn4*-GFP (**D**) RNAs with (“+”) or without *Cetn* MO (10 ng/side). These *Cetn* RNAs contain the target sequence of the corresponding morpholino. In addition, uninjected (“UN”) and embryos injected with GFP RNA alone were examined as controls for antibody specificity. Injected embryos were harvested at stage 11. Immunoblot analyses were carried out using an anti-rabbit GFP antibody. An apparent breakdown product of the *Cetn2*-GFP construct is indicated by the arrow in the *Cetn2* MO panel.

change in *Wnt8a* RNA levels (Fig. 4A). This is a pattern of changing RNA levels quite distinct from that observed in ectodermal explants and whole embryos injected with morpholinos directed against either of two other cilia/basal body-associated proteins, *Cby*<sup>22</sup> and *EFHC1* (Zhao *et al.*, in preparation). We

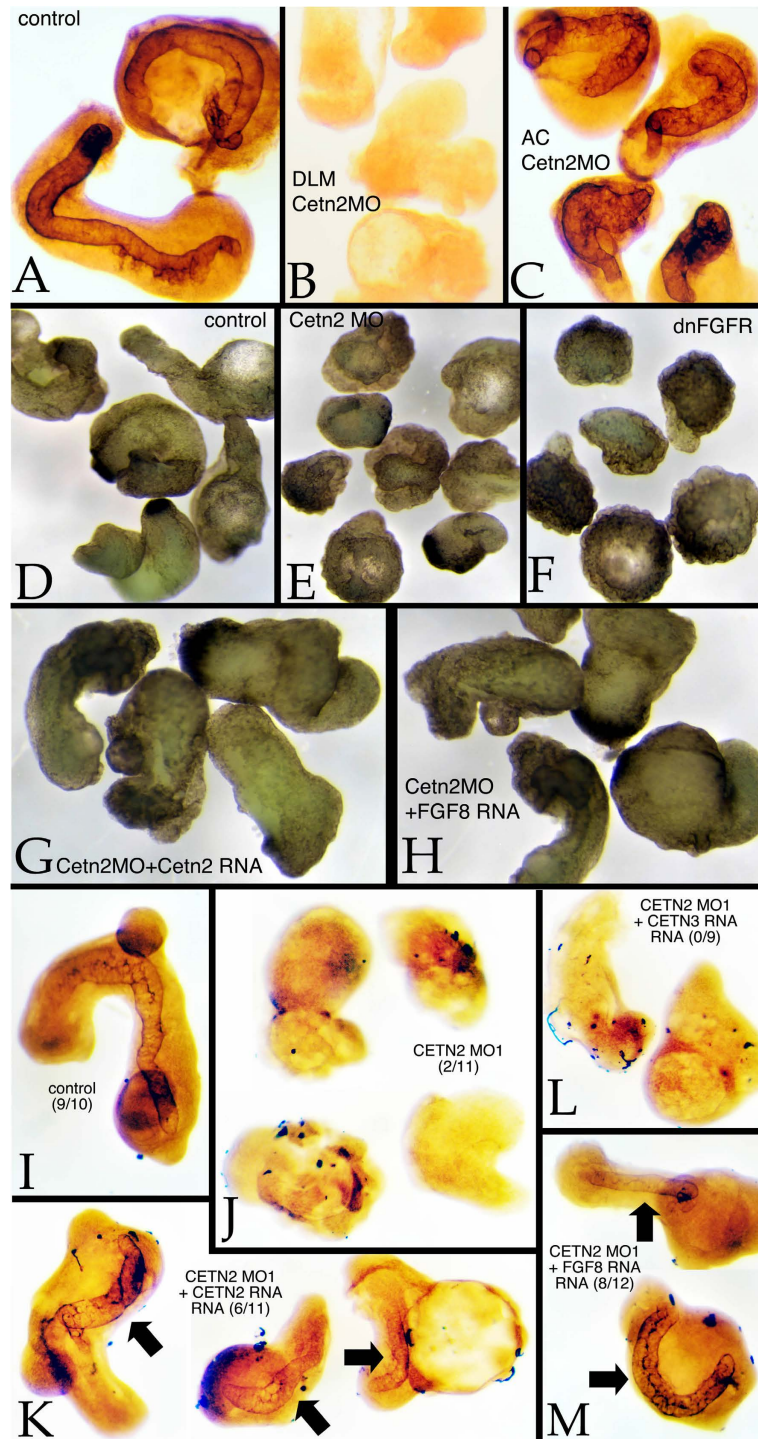


**Figure 3.** Animal cap/dorsal axial mesodermal zone (AC/DAMZ) explants were prepared from experimentally manipulated embryos when control (intact) embryos had reached stage 25. In wild type explants (A) staining with the anti-keratan sulfate antibody MZ15 revealed explant elongation and notochord formation. Both were absent in wild type AC/Cetrn2 morphant DAMZ explants (B). Notochord formation occurred in Cetrn2 morphant AC/wild type DAMZ explants (C). A comparison of dorsal axial mesoderm explant morphology (D-H) revealed the elongation of control explants (D), this elongation phenotype was absent in Cetrn2 morphant explants (E) and dominant-negative FGFR RNA injected explants (F). In Cetrn2 morphant explants, the elongation phenotype was rescued by either Cetrn2-GFP (G) or FGF8 (H) RNA injection (200 pgs/embryo). Morpholinos were injected at 10 ng/embryo. Staining with MZ15 revealed the presence of notochordal tissues in control (I) explants, its absence in Cetrn2 morphant explants (J), and its reappearance in Cetrn2 RNA (K) and FGF8 (M), but not in Cetrn3 RNA (L) injected Cetrn2 morphant explants - number of explants with notochord staining per total number of explants is presented in brackets in panels I-M.

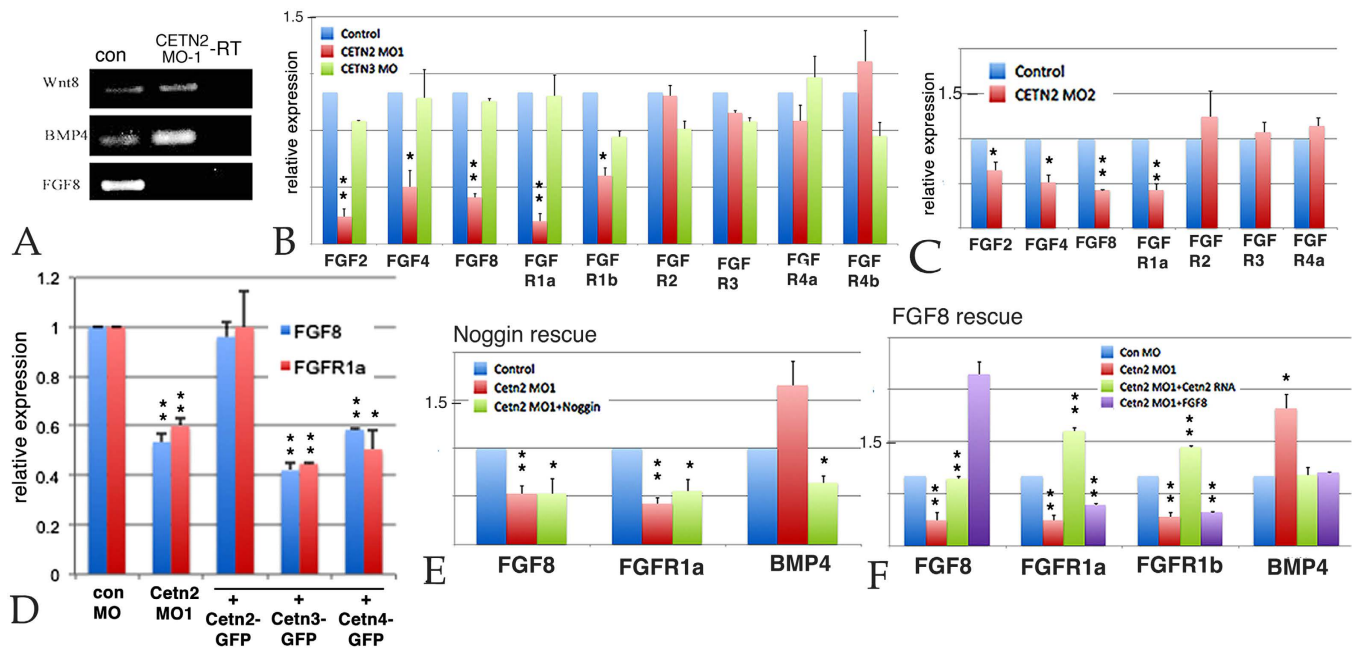


**Figure 4.** **A:** PCR analysis of control and *Cetn2* MO embryos; there was a clear increase in *BMP4* RNA, the disappearance of *FGF8* RNA, and no apparent effect on *Wnt8* RNA: **B:** qPCR analysis of Control, *Cetn2*MO1 and *Cetn3*MO embryos, injected in both cells of a two cell embryo and harvested at stage 11. **C:** A similar analysis carried out with the *Cetn2*MO2. **D:** qPCR analysis of embryos injected in both cells of a two cell embryo with *Cetn2*MO1 alone or together with *Cetn2*-GFP, *Cetn3*-GFP, or *Cetn4*-GFP RNAs (RNAs injected at 200 pg/side, total 400 pg/embryo; MOs injected at 10 ng/side, total 20 ng/embryo). While *Cetn2*-GFP RNA rescued the morphant phenotype *Cetn3* or *Cetn4* RNAs did not. **E:** qPCR analysis of embryos injected in both cells of two-cell embryos with *Cetn2*MO1 alone or together with *Noggin* RNA (200 pgs/embryo); *Noggin* reversed the morpholino effect on *BMP4* RNA level but not the effect on *FGF8* or *FGFR1a* RNA levels. **F:** qPCR analysis of embryos injected in both cells of a two cell embryo with *Cetn2*MO1 alone or together with either *Cetn2*-GFP or *FGF8* RNAs (200 pgs/embryo); *Cetn2* RNA rescued the *Cetn2* morpholino's effects on RNA levels, *FGF8* reversed the effect on *BMP4* RNA, but not the effects on *FGFR1a* RNAs. Levels of statistical significance indicated single \* <0.05, double \*\* <0.001.

confirmed this result using quantitative reverse transcription PCR (qPCR) of *Cetn2* morphant embryos prepared by injecting either the MO1 or MO2 *Cetn2* morpholinos. These morpholinos decreased the levels of *FGF2*, *FGF4*, *FGF8*, *FGFR1a*, and *FGFR1b* RNAs but produced no significant change in *FGFR2*, *FGFR3*, or *FGFR4a* RNAs. The *Cetn3* MO did not change the level of any *FGF* or *FGFR* RNA examined (Fig. 4B,C). In rescue studies, co-injection of *Cetn2*-GFP RNA could return the levels of *FGF8* and *FGFR1a* to control levels, while *Cetn3*-GFP and *Cetn4*-GFP RNAs could not (Fig. 4D).

FGF and BMP have been found to regulate each other's expression in the early embryo<sup>25</sup>. To determine whether the effects of *Cetn2* morpholinos were direct or indirect, we injected RNA encoding the BMP antagonist *Noggin*<sup>26</sup> into *Cetn2* morphant embryos. *Noggin* RNA reduced the *Cetn2* MO induced increase in the level of *BMP4a* RNA, but did not increase the level of *FGF8* RNA (Fig. 4E). In contrast, the injection of *FGF8* RNA reduced the *Cetn2* MO induced increase in the level of *BMP4a* RNA, but failed to rescue the levels of *FGFR1a* RNA (Fig. 4F). This suggests that *Cetn2* plays a direct role in the regulation of *FGF8* and *FGFR1a/b*, while its effects on *BMP4a* RNA levels are indirect and the result of changes in FGF signaling.

Given *Cetn2*'s established presence in the nucleus (see above) and the effects of the *Cetn2* morpholinos on *FGF8* and *FGFR1a* RNA levels, it seemed plausible that *Cetn2* might directly influence the expression of these genes through interactions with chromatin. We initially examined the *FGF8* gene in *X. tropicalis* using anti-XlCetn, anti-HsCetn1 (which preferentially reacts with *Cetn2* over *Cetn3* - see above), and anti-RNA polymerase II antibodies. We found that *Cetn* co-localized with polymerase at these loci (Fig. 5A). Further experiments in *X. laevis* used RNAs encoding GFP-tagged forms of *X. laevis* *Cetn2a*, *Cetn3l*, and *Cetn4* (see Methods). In ectodermal explants derived from RNA injected fertilized eggs, myc-*Cetn2*-GFP (Fig. 5B,C) and *Cetn4*-GFP (SupFig. 4) polypeptides preferentially accumulated in ciliated cells and localized to the basal body region of cilia (Fig. 5D,E). myc-*Cetn3*-GFP was also found to accumulate preferentially in ciliated cells (Fig. 5F,G) and was localized to basal bodies (Fig. 5H,I), but its localization was not quite as cilia-specific as that observed for *Cetn2*. That said, in ectodermal



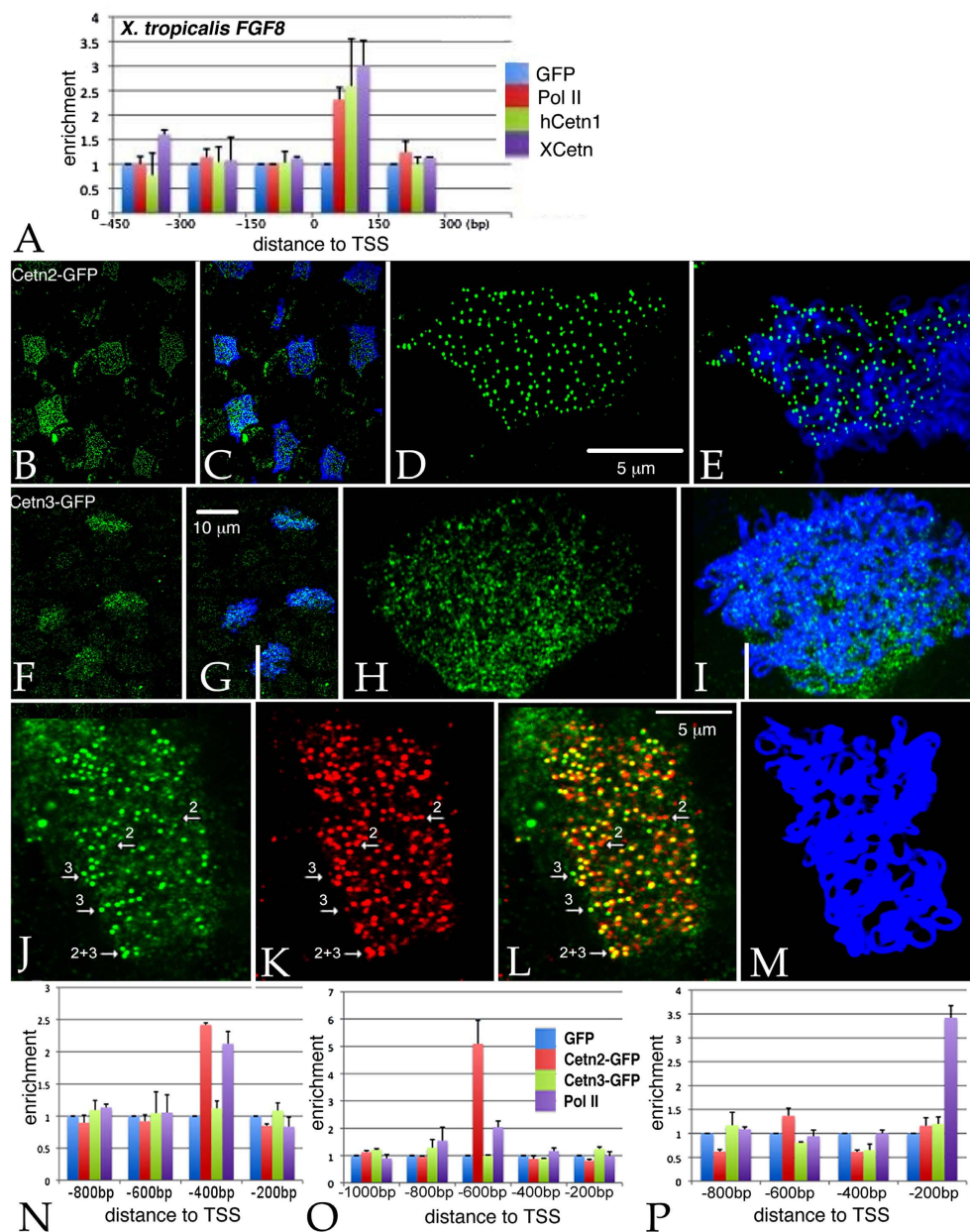


**Figure 5.** **A:** Unmanipulated *X. tropicalis* embryos were isolated at stage 11, subjected to ChIP using 2  $\mu$ g of either anti-GFP antibody (as control), anti-*Xenopus* Cetn antibody, anti-human Cetn1 antibody, or anti-Pol II antibodies. Isolated embryonic DNA was analyzed by qPCR using primers directed against the FGF8 promoter region. The distance from the transcription start site (TSS) is noted. For similar studies in *X. laevis*, we first characterized the behavior of the myc-Cetn2-GFP and myc-Cetn3-GFP polypeptides in ectodermal explants. Fertilized eggs were injected with encoding either myc-Cetn2-GFP RNA (**B-E**), myc-Cetn3-GFP RNA (**F-I**), or both Cetn2-RFP and myc-Cetn3-GFP RNAs (**K-M**) (each RNA injected at 200 pg/embryo). Ectodermal explants were isolated at stage 9 and fixed at stage 18. Immunofluorescence staining was performed using both anti-GFP and anti-AAT antibodies; scale bar in part **G** indicates 10  $\mu$ m for parts **B,C,F** and **G**. Scale bar in parts **D & L** indicates 5  $\mu$ m for parts **D,E,H,I** and **J-M**. Confocal images were taken at either 40X (**B,C,E,G**) or 100X (**D,E,H,I,J-M**) magnification. It is readily apparent that both myc-Cetn2-GFP and myc-Cetn3-GFP polypeptides accumulate in ciliated cells. In explants expressing both myc-Cetn3-GFP (**J**) and Cetn2-RFP (**K**; overlap in panel **L** is AAT staining), there was both extensive overlap in the localization of Cetn2 and Cetn3 polypeptides (arrow marked “2+3”), as well as sites where one or the other predominates (arrows marked either “2” or “3”). For ChIP studies in *X. laevis*, both blastomeres of 2-cell stage embryos were injected with RNAs encoding either GFP, myc-Cetn2-GFP, or myc-Cetn3-GFP; uninjected embryos were used as a control. Embryos were harvested at stage 11. GFP antibody was used to immunoprecipitate the injected embryos and Pol II antibody was used to immunoprecipitate the uninjected embryos. qPCR analysis was performed to check protein binding to the FGFR1a (**N**), FGF8 (**O**) and BMP4a (**P**) promoter regions.

explants expressing (from injected RNA) both a C-terminally RFP-tagged Cctn2 (Cctn2-RFP) and myc-Cctn3-GFP, we saw regions of high overlap, as well as regions of distinct Cctn2 and Cctn3 accumulation (Fig. 5J–M). In chromatin immunoprecipitation (ChIP) experiments, myc-Cctn2-GFP but not myc-Cctn3-GFP or GFP alone, co-localized with Pol II on the *FGF8* and *FGFR1a* genes (Fig. 5N,O); neither Cctn localized with Pol II on the *BMP4a* gene (Fig. 5P), as expected for an indirect target of Cctn2-mediated regulation.

Our work reveals a new and unexpected role for Cctn2 as a transcriptional regulator of a subset of FGF and FGFR genes. The fact that Cctn2 was found to co-localize with Pol II at some, but not all genes suggests that its promoter association is dependent upon the presence of other proteins. In addition to its nuclear role as part of the XPC DNA repair complex, Cctn2 has been reported to be an integral component of the Trex2 complex, which appears to interact with both nuclear pores and RNA polymerase and has been implicated in the nuclear export of mRNAs<sup>27,28</sup>. This suggests that the Cctn2 morphant phenotype could, in part, involve changes in Trex2 function or other, as yet unidentified interactions. To resolve this issue, we are currently in the process of identifying Cctn2-associated proteins in *Xenopus* and other systems.

The role of Cctn2 as a regulator of mesodermal differentiation, as revealed by notochord formation, in *Xenopus* early embryonic development may seem at odds with the reported phenotypes of morpholino treated Zebrafish embryos and Cctn2 null mice. In the Zebrafish *Danio rerio*, depletion of Cctn2 led to a ciliopathy-related cyst formation phenotype<sup>11</sup>. A syndromic ciliopathy, including dysosmia and hydrocephalus was reported in Cctn2 null mice<sup>12</sup>. We anticipate that the phenotypic differences between these three vertebrates can be attributed to differences in developmental mechanisms and Cctn2-containing complexes, the patterns of centrin gene expression during embryonic development, and perhaps some level of partial redundancy between the centrin genes, although neither Cctn3 or Cctn4 RNAs rescued the Cctn2 morphant gene expression phenotype. That said, a role of Cctn2 in the regulation of gene expression, and its integral role in the functions of XPC, Trex2, and perhaps other complexes, indicates the need for more subtle analyses of the physiological roles of Cctn2 in particular and Cctns as a class of proteins.

## Materials and Methods

**Embryos, their manipulation and analysis.** *X. laevis* embryos were staged, and explants were generated, following standard procedures<sup>29</sup>. Capped mRNAs were transcribed from linearized plasmid templates using mMessage mMachin kits (Ambion) following manufacturer's instructions. At the two-cell stage embryo injections were directed equatorially. As an injection tracer, we routinely included RNAs (150 pgs/embryo) encoding either  $\beta$ -galactosidase, green fluorescent protein (GFP) or GFP-CAAX, which is membrane-associated. In the case of GFP/GFP-CAAX RNA injection, embryos were examined at stage 10–11 by fluorescent microscopy to confirm the accuracy of injection. RNA isolation, cDNA synthesis, RT-PCR and qPCR analyses were carried out as described previously<sup>22,23</sup>. Real-time (quantitative) PCR was carried out using a Mastercycler Eppgradient Realplex device (Eppendorf). PCR reactions were set up using DyNAmo SYBR Green qPCR kits (Finnzymes). Each sample was normalized to the expression level of ornithine decarboxylase (ODC). The cycling conditions used were: 95°C for 5 minutes; then 40 cycles of 95°C for 15 seconds, 56°C for 15 seconds, 60°C for 30 seconds. The  $\Delta\Delta CT$  method was used to calculate real-time PCR results. The primers used for RT-PCR analysis were Ornithine decarboxylase (ODC) [U 5'-CAG CTA GCT GTG TGG-3' D 5'-CAA CAT GGA AAC TCA CAC-3']; Wnt8a [U 5'-TGA TGC CTT CAC TTC TGT GG-3' D 5'-TCC TGC AGC TTC TTC TCT CC -3']; BMP4 [U 5'-TGG TGG ATT AGT CTC GTG TCC -3' D 5'-TCA ACC TCA GCA GCA TTC C -3']; Noggin [U 5'-AGT TGC AGA TGT GGC TCT-3' D 5'-AGT CCA AGA GTC TCA GCA -3']; FGF8 [U 5'-TGG TGA CCG ACC AAC TAA GC D 5'-CGA TTA ACT TGG CGT GTG G ]; FGF2 [U 5'- AGA GGC TCT ACT GCA AGA ACG-3' D 5'- TTC CTT CAT GGC AAG GTA GC-3']; FGF4 [U 5'-GCA TGC CGT TCT CTT CTT CC -3' D 5'-ACG TCG CAG TCT CTT GAT GC -3']; FGFR1a [U 5'-GCG CAT TGG TGG ATA TAA GG -3' D 5'- AGA CCG GCT TGT AGG ATT GG-3']; FGFR1b [U 5'-GCG CAT TGG TGG ATA TAA GG -3' D 5'-GAG ACC GGC TTG TAG GAT AGG -3']; FGFR2 [U 5'- TCT GCA TGG TAG TGG TCT GC-3' D 5'- CAG GAG TCG TGT TGT GAT CC-3']; FGFR3 [U 5'- ACC AAG TGG TTC AAG GAT GG D 5'- TCG TCA TCC TCA TCA TCA CC]; FGFR4a [U 5'-ACA GTC AAG TTC CGC TGT CC -3' D 5'-GCT GCC AAC TCT GTT CTC TAC C -3']; and FGFR4b [U 5'-ACA CTG GAG CCT GGT AAT GG -3' D 5'-GCT ACC TAC ACG TGC TGT GG -3'].

**Morpholinos and plasmids.** Cctn coding sequences were isolated from maternal RNA by RT-PCR and subcloned into pCS2 plasmids, following protocols used previously to isolate Cby coding sequences<sup>22</sup>; where indicated such constructs had N-terminal myc and C-terminal GFP sequences<sup>30</sup>. We also generated plasmids that encode Cctn-GFP chimeras that either perfectly matched or were maximally mismatched to their respective morpholinos. Plasmids encoding either N- or C-terminally tagged Cctn2-RFP were obtained from Sergie Sokol (Mount Sinai School of Medicine) and John Wallingford (U. Texas, Austin). Plasmids encoding FGF8 and a dominant-negative form of FGFR1 were supplied by Enrique Amaya (U. Manchester). Morpholinos against *X. laevis* centrin were designed and synthesized by Gene Tools. These included two non-overlapping morpholinos against Cctn-2a [MO1 5'CTTG TAGTTAGAAGCCATATCACAC 3' and MO2 5'TGCACACACCAACCTTCGACCTCGC 3'], a Cctn-3l morpholino [5'CATCAGTCCTCACAGCCAGGCTCAT 3'], and a Cctn-4 morpholino



[5'CTGGTTTACGCAGAACAGAGGCCAT 3'](**supplemental figure. 2**). In each case, a NIH-Blast search of the morpholino sequence revealed only a single hit in *X. laevis*, namely the targeted *Cetn* RNA. A plasmid encoding membrane-bound GFP, GFP-CAAX, was supplied by Kristen Kwan (U. Utah). Statistical analyses were based on values expressed as mean  $\pm$  standard deviation and analyzed using the unpaired student's t-test.  $p < 0.05$  was considered as significant in all analyses.

**Immunocytochemistry and imaging.** Embryos were fixed and stained as described by Dent *et al.*<sup>31</sup>. The mouse monoclonal anti-acetylated  $\alpha$ -tubulin antibody was used to visualize ciliated cells<sup>32</sup>. The rabbit anti-Xenopus *Cetn* antibody (anti-XICetn) was supplied by Sergie Sokol<sup>20</sup>. The rabbit anti-human *Cetn1* antibody (anti-HsCetn1) was purchased from Sigma. The anti-HsCetn1 antibody is directed against the C-terminal 15 amino acids of *Cetn1*; a similar sequence exists at the C-termini of *X. laevis* *Cetn2* (13/15 identical) and *Cetn4* proteins (12/15 identical), but is absent from the *Cetn3* (5/15 identical)(data not shown). Notochord was visualized using the mouse monoclonal anti-keratin sulfate antibody MZ15 obtained from the Developmental Studies Hybridoma Bank<sup>33</sup>. Immunoperoxidase-stained explants were bleached before staining while immunofluorescently-labeled embryos were not. Fluorescent images were collected using a Zeiss 510 Confocal Laser Scanning Microscope.

**ChIP studies.** Chromatin immunoprecipitation (ChIP) was performed following the protocol described in Blythe *et al.*<sup>34</sup>. Briefly, at stage 11 uninjected embryos, or embryos injected with GFP, CETN2-GFP, or CETN3-GFP RNAs were cross-linked with 1% formaldehyde for 30 minutes; cross-linking was stopped with a 10 min wash in 0.125M Glycine/PBS, followed by three washes in PBS. Samples were resuspended in RIPA buffer (50 mM Tris-HCl, pH 7.4, 1% NP-40 (Sigma I3021), 0.25% Na-Deoxycholate, 150 mM NaCl, 1 mM EDTA, 0.1% SDS, 0.5 mM DTT, 5 mM Na-Butyrate, Protease Inhibitor Cocktail (Sigma P8340), Phosphatase Inhibitor Cocktail I (Sigma P2850), Phosphatase Inhibitor Cocktail II (Sigma P5726). Chromatin was sonicated on ice to an average size of 200-500 base pairs using a Bioruptor (Diagenode). Immunoprecipitation was performed using Dynabeads Protein G (Life Technologies) coupled to 2  $\mu$ g GFP antibody (ICL, Inc) or Pol II antibody (Diagenode) at 4°C overnight. The bound chromatin was eluted and cross-links were reversed at 65°C overnight. ChIP DNA was extracted with phenol-chloroform and qPCR was performed. Below is a list of the primers used in ChIP studies. *X. tropicalis* CHIP primers: Fgf8 [primer 1 U 5'- TGA CTT TGC GCT CTG ACT TT-3' D 5'- AAA AGA AAC AGC CGA GAT GC-3']; [primer 2 U 5'- GCA TCT CGG CTG TTT CTT TT -3' D 5'- GAT AGT GAT GGG GAG AGC CT -3']; [primer 3 U 5'- CAGGCTCTCCCCATCACTAT -3' D 5'- GAG TAG AAA CAC GCT GCA CT-3']; [primer 4 U 5'- CCT CTC TTC CAG ACT CGG CT -3' D 5'- GGA GTC GGA TTG CAG TGG AG-3']; [primer 5 U 5'-TGA GCT ACA TCA CCT CCA TC-3' D 5'-GAA GAG AAG GTC CAG TTA GCA -3']. *X. laevis* CHIP primers: FGFR1a [primer 1 U 5'-ACA GAG TGG CAA TTA TAC AGA GG -3' D 5'-CAC CTC ACA GCC ACA ATA CC -3']; [primer 2 U 5'-GAG AGG CTG TGA GCA TAA TGG-3' D 5'-TGC TAC TAT AGG CAC CAT CAC C-3']; [primer 3 U 5'-GGA GAG AGA TGG TGC CTA TGG -3' D 5'-TCT TCC TAC TAC ACT TGC TGT CC-3']; [primer 4 U 5'-TGG TGC CTA TAG TAG CAG TGG -3' D 5'-CTC CAG AGC ACA AGC ATG G-3']; FGF8 [primer 1 U 5'-CAC TCA CAC TGT GTC TCT CAG G -3' D 5'-CCG GCC AAT AAC ACT AGA AGC-3']; [primer 2 U 5'-TCA GCT CAG ACA CAC CAA GC -3' D 5'-TTC TCT CTC TCT CTC GCT TCC -3']; [primer 3 U 5'- TCA GCT CAG ACA CAC CAA GC -3' D 5'- CAA GGA GGC GAG TTA CTT CC -3']; [primer 4 U 5'- AGT AAC TCG CCT CCT TGT CG -3' D 5'- GCC TCT CAA GAG CAA GAT GC -3']; [primer 5 U 5'- GAC AGT AGC GCA ACA CTC G -3' D 5'- GCC TCT CAA GAG CAA GAT GC -3']; BMP4a [primer 1 U 5'- TTG GCT GTC AAG AAT CAT GG -3' D 5'- CAG CAG GAA GTA GCC AGA GC -3']; [primer 2 U 5'- ACA CGG CTC TGG CTA CTT CC -3' D 5'- AGC CTG GCC AAT GAA TGC -3']; [primer 3 U 5'- GGA CAT ATC GCA GGC TAT CG -3' D 5'- TCA GAT AGT CAC CGC CAT CC -3']; [primer 4 U 5'- GAG ACG CTC TCA GTC AGA TTA GC -3' D 5'- CAA GGA CAG TTC CAC AGA GG -3'].

**Note added in proof:** Recently, human centrin 2 has been shown to regulate primary cilia formation through controlling CP110<sup>35</sup>.

## References

- Hartman, H. & Fedorov, A. The origin of the eukaryotic cell: a genomic investigation. *Proceedings of the National Academy of Sciences* **99**, 1420–1425 (2002).
- Friedberg, F. Centrin isoforms in mammals. Relation to calmodulin. *Mol. Biol. Rep.* **33**, 243–252, doi:10.1007/s11033-006-9004-z (2006).
- Dantas, T. J., Daly, O. M. & Morrison, C. G. Such small hands: the roles of centrins/caltractins in the centriole and in genome maintenance. *Cell Mol. Life Sci.*, doi:10.1007/s00018-012-0961-1 (2012).
- Baum, P., Furlong, C. & Byers, B. Yeast gene required for spindle pole body duplication: homology of its product with Ca2+ -binding proteins. *Proc. Natl. Acad. Sci. USA* **83**, 5512–5516 (1986).
- Stemm-Wolf, A. J. *et al.* Basal body duplication and maintenance require one member of the Tetrahymena thermophila centrin gene family. *Mol. Biol. Cell* **16**, 3606–3619, doi:E04-10-0919 (2005).
- Vonderfecht, T. *et al.* The two domains of centrin have distinct basal body functions in Tetrahymena. *Mol. Biol. Cell* **22**, 2221–2234, doi:mbc.E11-02-0151 (2011).
- Vonderfecht, T., Cookson, M. W., Giddings, T. H., Jr., Clarissa, C. & Winey, M. The two human centrin homologues have similar but distinct functions at Tetrahymena basal bodies. *Mol. Biol. Cell* **23**, 4766–4777, doi:mbc.E12-06-0454 (2012).

8. Hart, P. E., Glantz, J. N., Orth, J. D., Poynter, G. M. & Salisbury, J. L. Testis-Specific Murine Centrin, Cctn1: Genomic Characterization and Evidence for Retroposition of a Gene Encoding a Centrosome Protein. *Genomics* **60**, 111–120 (1999).
9. Zhu, J. *et al.* Comparative genomics search for losses of long-established genes on the human lineage. *PLoS computational biology* **3**, e247 (2007).
10. Avasthi, P. *et al.* Germline deletion of Cctn1 causes infertility in male mice. *Journal of cell science* **126**, 3204–3213 (2013).
11. Delaval, B., Covassin, L., Lawson, N. D. & Doherty, S. Centrin depletion causes cyst formation and other ciliopathy-related phenotypes in zebrafish. *Cell Cycle* **10**, 3964–3972, doi:18150 (2011).
12. Ying, G. *et al.* Centrin 2 Is Required for Mouse Olfactory Ciliary Trafficking and Development of Ependymal Cilia Planar Polarity. *The Journal of Neuroscience* **34**, 6377–6388 (2014).
13. Dantas, T. J., Wang, Y., Lalor, P., Dockery, P. & Morrison, C. G. Defective nucleotide excision repair with normal centrosome structures and functions in the absence of all vertebrate centris. *J. Cell Biol.* **193**, 307–318, doi:jcb.201012093 (2011).
14. Araki, M. *et al.* Centrosome protein centrin 2/caltractin 1 is part of the xeroderma pigmentosum group C complex that initiates global genome nucleotide excision repair. *J. Biol. Chem.* **276**, 18665–18672, doi:10.1074/jbc.M100855200 (2001).
15. Nishi, R. *et al.* Centrin 2 stimulates nucleotide excision repair by interacting with xeroderma pigmentosum group C protein. *Mol. Cell Biol.* **25**, 5664–5674, doi:25/13/5664 (2005).
16. Paoletti, A., Moudjou, M., Paintrand, M., Salisbury, J. L. & Bornens, M. Most of centrin in animal cells is not centrosome-associated and centrosomal centrin is confined to the distal lumen of centrioles. *J. Cell Sci.* **109** ( Pt 13), 3089–3102 (1996).
17. Sive, H. 'Model' or 'tool'? New definitions for translational research. *Dis. Model Mech.* **4**, 137–138, doi:4/2/137 (2011).
18. James-Zorn, C. *et al.* Xenbase: expansion and updates of the *Xenopus* model organism database. *Nucleic acids research* **41**, D865–D870 (2013).
19. Yanai, I., Peshkin, L., Jorgensen, P. & Kirschner, M. W. Mapping gene expression in two *Xenopus* species: evolutionary constraints and developmental flexibility. *Dev. Cell* **20**, 483–496, doi:S1534-5807(11)00121-3 (2011).
20. Kim, K. D., Lake, B. B., Harembaki, T., Weinstein, D. C. & Sokol, S. Y. Rab11 regulates planar polarity and migratory behavior of multiciliated cells in *Xenopus* embryonic epidermis. *Developmental Dynamics* **241**, 1385–1395 (2012).
21. Amaya, E., Stein, P. A., Musci, T. J. & Kirschner, M. W. FGF signalling in the early specification of mesoderm in *Xenopus*. *Development* **118**, 477–487 (1993).
22. Shi, J., Zhao, Y., Galati, N., Winey, M. & Klymkowsky, M. W. Chibby functions in *Xenopus* ciliary assembly, embryonic development, and the regulation of gene expression. *Dev. Biol.* **395**, 287–298, doi:10.1016/j.ydbio.2014.09.008 (2014).
23. Shi, J., Severson, C., Yang, J., Wedlich, D. & Klymkowsky, M. W. Snail2 controls BMP/Wnt mesodermal induction of neural crest. *Development* **138**, 3135–3145, doi:10.1242/dev.064394 (2011).
24. Smith, J. C. Forming and interpreting gradients in the early *Xenopus* embryo. *Cold Spring Harb. Perspect Biol.* **1**, a002477, doi:10.1101/cshperspect.a002477 (2009).
25. Delaune, E., Lemaire, P. & Kodjabachian, L. Neural induction in *Xenopus* requires early FGF signalling in addition to BMP inhibition. *Development* **132**, 299–310 (2005).
26. Zimmerman, L. B., De Jesus-Escobar, J. M. & Harland, R. M. The Spemann organizer signal noggin binds and inactivates bone morphogenetic protein 4. *Cell* **86**, 599–606 (1996).
27. Jani, D. *et al.* Functional and structural characterization of the mammalian TREX-2 complex that links transcription with nuclear messenger RNA export. *Nucleic acids research* **40**, 4562–4573 (2012).
28. Cunningham, C. N., Schmidt, C. A., Schramm, N. J., Gaylord, M. R. & Resendes, K. K. Human TREX2 components PCID2 and centrin 2, but not ENY2, have distinct functions in protein export and co-localize to the centrosome. *Experimental cell research* **320**, 209–218 (2014).
29. Nieuwkoop, P. D. & Faber, J. *Normal table of Xenopus laevis (Daudin): A Systematical and Chronological Survey of the Development from the Fertilized Egg till the end of Metamorphosis.* (Amsterdam Publishing Company, republished in 1994 by Garland Publishing, 1967).
30. Rubenstein, A., Merriam, J. & Klymkowsky, M. W. Localizing the adhesive and signaling functions of plakoglobin. *Dev. Genet.* **20**, 91–102 (1997).
31. Dent, J. A. & Klymkowsky, M. W. *Whole-mount analyses of cytoskeletal reorganization and function during oogenesis and early embryogenesis in Xenopus.* (Academic Press, 1989).
32. Chu, D. T. W. & Klymkowsky, M. W. The appearance of acetylated alpha-tubulin during early development and cellular differentiation in *Xenopus*. *Dev. Biol.* **136**, 104–117 (1989).
33. Smith, J. C. & Watt, F. M. Biochemical specificity of *Xenopus* notochord. *Differentiation* **29**, 109–115 (1985).
34. Blythe, S. A., Reid, C. D., Kessler, D. S. & Klein, P. S. Chromatin immunoprecipitation in early *Xenopus laevis* embryos. *Dev. Dyn.* **238**, 1422–1432, doi:10.1002/dvdy.21931 (2009).
35. Prosser, S. L. & Morrison, C. G. Centrin2 regulates CP110 removal in primary cilium formation. *J Cell Biol.* **208**, 693–701 (2015).

## Acknowledgements

We thank Nick Galati with help with confocal imaging, Sergei Sokol for anti-centrin antibody; plasmids were obtained from Sergie Sokol, John Wallingford, Kris Kwon, Enrique Amaya, and Richard Harland. The work was supported by NIH grant GM74746 (and supplement) to MW and in part through GM84133 to MWK.

## Author Contributions

Together J.S. and M.W.K. designed the *Xenopus* studies, J.S. performed the bulk of the *Xenopus* studies, with the assistance of Y.Z., T.V. was involved in the original isolation of *X. laevis* centrin cDNAs, M.W.K. performed the explant staining studies and J.S., M.W. and M.W.K. were involved in overall project design and manuscript preparation.

## Additional Information

**Supplementary information** accompanies this paper at <http://www.nature.com/srep>

**Competing financial interests:** The authors declare no competing financial interests.

**How to cite this article:** Shi, J. *et al.* Centrin-2 (Cctn2) mediated regulation of FGF/FGFR gene expression in *Xenopus*. *Sci. Rep.* **5**, 10283; doi: 10.1038/srep10283 (2015).



This work is licensed under a Creative Commons Attribution 4.0 International License. The images or other third party material in this article are included in the article's Creative Commons license, unless indicated otherwise in the credit line; if the material is not included under the Creative Commons license, users will need to obtain permission from the license holder to reproduce the material. To view a copy of this license, visit <http://creativecommons.org/licenses/by/4.0/>